

Daniele de Sanctis,^{a*} Isabel Bento,^a José Manuel Inácio,^a Sónia Custódio,^a Isabel de Sá-Nogueira^{a,b} and Maria Arménia Carrondo^a

^aInstituto de Tecnologia Química e Biológica, Universidade Nova de Lisboa, Avenida da República—EAN, 2780-157 Oeiras, Portugal, and ^bFaculdade de Ciências e Tecnologia, Universidade Nova de Lisboa, Quinta da Torre, 2829-516 Caparica, Portugal

Correspondence e-mail: desanctisd@gmail.com

Received 17 April 2008
Accepted 29 May 2008

Overproduction, crystallization and preliminary X-ray characterization of Abn2, an endo-1,5- α -arabinanase from *Bacillus subtilis*

Two *Bacillus subtilis* extracellular endo-1,5- α -L-arabinanases, AbnA and Abn2, belonging to glycoside hydrolase family 43 have been identified. The recently characterized Abn2 protein hydrolyzes arabinan and has low identity to other reported 1,5- α -L-arabinanases. Abn2 and its selenomethionine (SeMet) derivative have been purified and crystallized. Crystals appeared in two different space groups: *P*1, with unit-cell parameters $a = 51.9$, $b = 57.6$, $c = 86.2$ Å, $\alpha = 82.3$, $\beta = 87.9$, $\gamma = 63.6^\circ$, and *P*₂₁₂₁₂₁, with unit-cell parameters $a = 57.9$, $b = 163.3$, $c = 202.0$ Å. X-ray data have been collected for the native and the SeMet derivative to 1.9 and 2.7 Å resolution, respectively. An initial model of Abn2 is being built in the SeMet-phased map.

1. Introduction

Arabinan is an L-arabinose homoglycan present in plant tissues that is generally associated with pectins. This polysaccharide is composed of α -1,5-linked L-arabinofuranosyl units, some of which are substituted with α -1,3- and α -1,2-linked chains of L-arabinofuranosyl residues (Beldman *et al.*, 1997). The two major enzyme families that hydrolyse arabinan are α -L-arabinofuranosidases (EC 3.2.1.55; AFs) and endo-1,5- α -L-arabinanases (EC 3.2.1.99; ABNs). AFs remove arabinose side chains, allowing ABNs to attack the glycosidic bonds of the arabinan backbone, releasing a mixture of arabino-oligosaccharides and L-arabinose as the products of the reaction. Arabinanases have several applications, in particular in the food industry, such as food technology and nutritional medical research (Beldman *et al.*, 1997).

Bacillus subtilis, a Gram-positive endospore-forming bacterium which participates in plant-biomass degradation, synthesizes two extracellular ABNs belonging to glycoside hydrolase family 43 (GH43; Coutinho & Henrissat, 1999), AbnA and Abn2 (YxiA), which hydrolyze sugar-beet arabinan (branched), linear α -1,5-L-arabinan and pectin (Inácio & de Sá-Nogueira, 2008; Leal & de Sá-Nogueira, 2004). The three-dimensional structures of three different 1,5- α -L-arabinanases, Arb43A from *Cellvibro japonicus* (Nurizzo *et al.*, 2002), BsArb43A (AbnA) from *B. subtilis* (Proctor *et al.*, 2005) and ABN-TS from *B. thermodenitrificans* (Yamaguchi *et al.*, 2005), have been determined by X-ray crystallography. These enzymes, which vary in length from 323 to 347 amino acids, display a unique motif consisting of a five-bladed β -propeller fold. Since the recently characterized Abn2 from *B. subtilis* (Inácio & de Sá-Nogueira, 2008) shows less than 23% amino-acid identity to these 1,5- α -L-arabinanases and is a much larger enzyme (469 residues) than other related arabinanases, the determination of its three-dimensional structure should provide valuable information concerning the structural features of glycoside hydrolase family 43 arabinanases. Here, we report the crystallization and preliminary X-ray analysis of the GH family 43 Abn2 from *B. subtilis*.

2. Experimental procedures

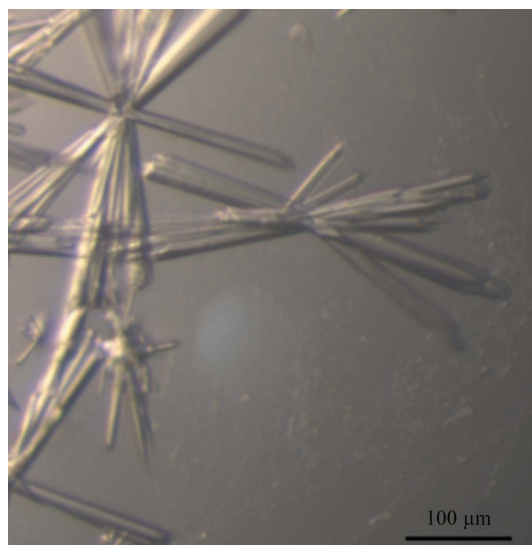
2.1. Overproduction and purification

The overproduction and purification of Abn2 in *Escherichia coli* BL21 (DE3) pLysS has been described previously (Inácio & de Sá-Nogueira, 2008). Briefly, the *abn2* allele (GenBank accession No.

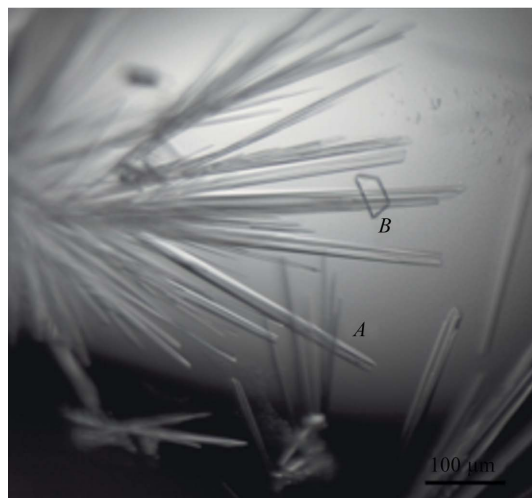


EU373814) was amplified by PCR with primers ARA237 (5'-GGC-GAATTGTTCAATATGTTCAACCG-3') and ARA238 (5'-CGCTT-CTCCCTCGAGTTTAGATCCC-3') using chromosomal DNA of wild-type strain *B. subtilis* 168 T⁺ as template. The resulting 1568 bp DNA fragment was digested with *NdeI*-*XhoI* unique restriction sites introduced by the primers (bold sequence) and cloned into the same sites of pET30a(+) (Novagen). In the resulting plasmid pZI39, the wild-type primary sequence of the Abn2 is fused directly to the carboxyl-terminal sequence (LEHHHHHH) encoded by pET30a(+).

E. coli BL21 (DE3) pLysS cells harbouring pZI39 were grown at 310 K and 160 rev min⁻¹ in 1 l LB with an appropriate antibiotic selection. When the OD₆₀₀ reached 0.6, expression of Abn2 was induced by the addition of 1 mM IPTG. The culture was grown for an additional 4 h at 310 K and 160 rev min⁻¹. Cells were harvested by centrifugation at 277 K and 8000g for 10 min. All subsequent steps were carried out at 277 K. The periplasmic protein fraction (PPF) was prepared by osmotic shock and loaded onto a 1 ml HisTrap column (Amersham Pharmacia Biotech). The Ni-bound proteins were eluted



(a)



(b)

Figure 1

(a) SeMet-derivative crystals of Abn2. The dimensions of a typical crystal fragment used in data collection were $0.05 \times 0.05 \times 0.2$ mm. (b) Crystals of the native Abn2 crystals. Two crystalline forms are present. Crystal form A belongs to space group *P1* and has typical dimensions of $0.02 \times 0.06 \times 0.1$ mm; crystal form B belongs to space group *P2₁2₁2₁*.

Table 1

Data-collection and processing statistics.

Values in parentheses are for the highest resolution shell.

	SeMet	Wild type
Wavelength (Å)	0.97865	1.03320
Space group	<i>P2₁2₁2₁</i>	<i>P1</i>
Unit-cell parameters (Å, °)	<i>a</i> = 57.9, <i>b</i> = 163.3, <i>c</i> = 202.0	<i>a</i> = 51.9, <i>b</i> = 57.6, <i>c</i> = 86.2, α = 82.3, β = 87.9, γ = 63.6
Resolution limits (Å)	127.0–2.70 (2.85–2.70)	85.4–1.90 (2.00–1.90)
$R_{\text{merge}}^{\dagger}$	0.093 (0.190)	0.047 (0.136)
$R_{\text{p.i.m.}}^{\ddagger}$	0.056 (0.121)	0.045 (0.036)
Total No. of reflections	365808 (46766)	134405 (17357)
No. of unique reflections	53601 (7661)	67116 (8980)
Mean $I/\sigma(I)$	17.6 (7.4)	14.5 (6.4)
Completeness (%)	99.9 (99.6)	95.7 (87.1)
Multiplicity	6.8 (6.1)	2.0 (1.9)
R_{ano}^{\S}	0.064 (0.112)	
Anomalous completeness (%)	99.1 (95.0)	
Anomalous multiplicity	3.5 (3.2)	

[†] $R_{\text{merge}} = \frac{\sum_{hkl} \sum_i |I_i(hkl) - \langle I(hkl) \rangle|}{\sum_{hkl} \sum_i I_i(hkl)}$. [‡] $R_{\text{p.i.m.}} = \frac{\sum_{hkl} [N/(N-1)]^{1/2} \sum_i |I_i(hkl) - \langle I(hkl) \rangle|}{\sum_{hkl} \sum_i I_i(hkl)}$. [§] $R_{\text{ano}} = \frac{\sum_h |I(h) - \langle I(-h) \rangle|}{\sum_h [I(h) + \langle I(-h) \rangle]}$, where $\langle I(h) \rangle$ indicates the mean intensity of symmetry-related reflections of the same Bijvoet mates *h*.

with a discontinuous imidazole gradient and fractions containing Abn2 that were more than 95% pure were dialyzed overnight against a buffer containing 100 mM Tris pH 8.0, 100 mM NaCl, 10% (v/v) glycerol. Purified protein was then concentrated using an Amicon Ultra 15 Centrifugal filter (Millipore) to a final concentration of 10.9 mg ml⁻¹ and stored in the same buffer at 193 K. Seleno-L-methionine-labelled protein was overexpressed in an auxotrophic *E. coli* strain B834 (DE3) harbouring pZI39. A colony was used to inoculate 10 ml LB with an appropriate antibiotic selection and the culture was incubated for 6 h at 150 rev min⁻¹ and 310 K. The culture was then diluted in a 1:20 ratio with 100 ml of SeMet Base media (Molecular Dimensions Ltd), L-methionine, Nutrient Mix (Molecular Dimensions Ltd) and an appropriate antibiotic selection. After overnight incubation the cell pellet was separated by centrifugation at 3000g and 298 K for 10 min, washed to remove residual L-methionine and resuspended in 1 l of the same medium containing L-seleno-methionine (SeMet; Molecular Dimensions Ltd) instead of L-methionine. When the OD₆₀₀ reached 0.75, induction was performed by the addition of 1 mM IPTG. The culture was grown for an additional 3 h and cells were then harvested. Preparation of the PPF and purification of SeMet-Abn2 was carried out as described above for the native protein. Purified protein was concentrated to a final concentration of 15.4 mg ml⁻¹ using an Amicon Ultra 15 Centrifugal filter (Millipore) and stored in the same buffer as the native protein at 193 K.

2.2. Crystallization

Preliminary crystallization screens were carried out with the native protein using a sitting-drop vapour-diffusion experimental setup (100 nl protein solution added to 100 nl reservoir solution equilibrated against 100 μ l reservoir solution) using a Cartesian Nanodrop Robot to set up 96-well plates at 294 K. Crystals were found in condition No. 22 [0.1 M HEPES pH 7.5, 70% (v/v) MPD] of Classics Screen (Nextal). Crystal growth was scaled up by hanging-drop vapour diffusion at 294 K in 48-well plates (1 μ l protein solution and 1 μ l reservoir solution equilibrated against 200 μ l reservoir solution), obtaining the best shaped crystals in 65% (v/v) MPD, 0.1 M Tris pH 8.5. The crystals that appeared showed two distinct morphologies (Fig. 1). Final crystal dimensions were $40 \times 50 \times 200$ μ m for crystal form A and $20 \times 60 \times 100$ μ m for crystal form B. The SeMet-protein

crystallization experiment was set up using the same conditions as used for the native protein, but crystals appeared only in one crystalline form (Fig. 1). The best-shaped crystals were obtained with 62% (v/v) MPD and 0.1 M Tris pH 8.4.

2.3. X-ray analysis

Crystals were transferred into a stabilizing solution containing 70% (v/v) MPD and 0.1 M Tris pH 8.5 and subsequently flash-cooled in liquid nitrogen. Native protein crystals with different morphologies belonged to different space groups: crystal form *A* belonged to space group $P2_12_12_1$, with unit-cell parameters $a = 57.81$, $b = 164.48$, $c = 203.31$ Å, and can accommodate four molecules in the asymmetric unit with a Matthews coefficient $V_M = 2.29$ Å³ Da⁻¹ and a solvent content of 46%, while crystal form *B* belonged to space group $P1$, with unit-cell parameters $a = 51.97$, $b = 57.64$, $c = 86.27$ Å, $\alpha = 82.31$, $\beta = 87.97$, $\gamma = 63.66^\circ$, which is compatible with the presence of two molecules in the asymmetric unit, corresponding to a Matthews coefficient $V_M = 2.17$ Å³ Da⁻¹ and a solvent content of 43% (Matthews, 1985). As the $P1$ crystals were the better diffracting crystal form, a data set was collected from these native crystals to 1.9 Å resolution at ID29, ESRF (Grenoble) at 100 K in 180 non-overlapping 1° oscillation images with a crystal-to-detector distance of 265.56 mm. Data were indexed with *MOSFLM* (Leslie, 2006) and scaled with *SCALA* (Evans, 2006).

The SeMet derivative of Abn2 only crystallized in one crystal form, which was similar to form *A* of the wild-type protein. SeMet-derivative crystals diffracted to 2.7 Å resolution and belonged to space group $P2_12_12_1$, with unit-cell parameters $a = 57.84$, $b = 163.22$, $c = 201.85$ Å, which can accommodate four molecules (each containing 13 selenomethionine residues) in the asymmetric unit, corresponding to a Matthews coefficient of 2.26 Å³ Da⁻¹ and a solvent content of 46%.

SAD data were collected from an SeMet-labelled crystal at 100 K at the BM14 Station at ESRF at a wavelength of 0.97865 Å, which was chosen after an absorption scan measurement to maximize the anomalous signal of Se atoms. Oscillation steps of 0.2° over a range of 180° were applied with a crystal-to-detector distance of 291.89 mm. SeMet-derivative crystal diffraction images were indexed with *MOSFLM* (Leslie, 2006) and scaled with *SCALA* (Evans, 2006).

2.4. Structure solution

The program *SOLVE* (Terwilliger & Berendzen, 1999) was used to locate 31 of the 42 Se atoms in the asymmetric unit and to perform initial phasing to a figure of merit of 33% (*Z* score 54.3). Subsequently, *RESOLVE* (Terwilliger, 2000) was used to perform statistical density modification with noncrystallographic symmetry averaging to a final figure of merit of 72%. In the final map, autotracing using *RESOLVE* (Terwilliger, 2003) succeeded in building some main features of the four independent molecules in the asymmetric unit, resulting in the placement of 765 residues out of 1876. Manual model building with *Coot* (Emsley & Cowtan, 2004) is in progress.

This work was partially supported by grant No. POCI/AGR/60236/2004 from Fundação para a Ciência e Tecnologia (FCT) and FEDER to IdS-N and fellowship SFRH/BD/18238/2004 from FCT to JMI.

References

- Beldman, G., Schols, H. A., Pitson, S. M., Searle-van Leeuwen, M. J. F. & Voragen, A. G. J. (1997). *Advances in Macromolecular Carbohydrate Research*, Vol. 1, edited by R. J. Sturgeon, pp. 1–64. Stamford: JAI Press.
- Coutinho, P. M. & Henrissat, B. (1999). *Recent Advances in Carbohydrate Bioengineering*, edited by H. J. Gilbert, G. J. Davies, B. Henrissat & B. Svensson, pp. 3–12. Cambridge: The Royal Society of Chemistry.
- Emsley, P. & Cowtan, K. (2004). *Acta Cryst.* **D60**, 2126–2132.
- Evans, P. (2006). *Acta Cryst.* **D62**, 72–82.
- Inácio, J. M. & de Sá-Nogueira, I. (2008). *J. Bacteriol.* **190**, 4272–4280.
- Leal, T. F. & de Sá-Nogueira, I. (2004). *FEMS Microbiol. Lett.* **241**, 41–48.
- Leslie, A. G. W. (2006). *Acta Cryst.* **D62**, 48–57.
- Matthews, B. W. (1985). *Methods Enzymol.* **114**, 176–187.
- Nurizzo, D., Turkenburg, J. P., Charnock, S. J., Roberts, S. M., Dodson, E. J., McKie, V. A., Taylor, E. J., Gilbert, H. J. & Davies, G. J. (2002). *Nature Struct. Biol.* **9**, 665–668.
- Proctor, M. R., Taylor, E. J., Nurizzo, D., Turkenburg, J. P., Lloyd, R. M., Vardakou, M., Davies, G. J. & Gilbert, H. J. (2005). *Proc. Natl Acad. Sci. USA*, **102**, 2697–2702.
- Terwilliger, T. C. (2000). *Acta Cryst.* **D56**, 965–972.
- Terwilliger, T. C. (2003). *Acta Cryst.* **D59**, 38–44.
- Terwilliger, T. C. & Berendzen, J. (1999). *Acta Cryst.* **D55**, 849–861.
- Yamaguchi, A., Tada, T., Wada, K., Nakaniwa, T., Kitatani, T., Sogabe, Y., Takao, M., Sakai, T. & Nishimura, K. (2005). *J. Biochem.* **137**, 587–592.